Photoinduced Electron and Energy Transfer Processes in a Bichromophoric Pyrene−Perylene Bisimide System

Başak Kükrer Kaletaş,[†] Rainer Dobrawa,[‡] Armin Sautter,[‡] Frank Würthner,*[,‡] Mikhail Zimine,[†] Luisa De Cola,[†] and René M. Williams*[,†]

Molecular Photonic Materials, van 't Hoff Institute for Molecular Sciences, Universiteit van Amsterdam, Nieuwe Achtergracht 166, 1018 WV Amsterdam, The Netherlands, and Institut für Organische Chemie, Universität Würzburg, Am Hubland, D-97074 Würzburg, Germany

Received: October 29, 2003; In Final Form: January 13, 2004

The synthesis and photophysical properties of a system consisting of a bay-functionalized perylene bisimide, containing four appended pyrene and two coordinating pyridine units, and its reference system are described. A complete study of their photophysical properties was obtained using UV−vis absorption, steady state and time-resolved emission, and femtosecond transient absorption. Analysis of the data, obtained from time-resolved emission and femtosecond transient absorption spectroscopy, showed the presence of both photoinduced electron and energy transfer processes. A high yield (>90%) and fast photoinduced energy transfer ($k_{en} \approx 6.2 \times 10^9$ s^{-1}) is followed by efficient electron transfer (70%, $k_{et} \approx 6.6 \times 10^9$ s^{-1}) from the pyrene units to the perylene bisimide moiety. The energy donor−acceptor distance, $R = 8.6$ Å, is calculated from the experimental energy transfer rate using Förster theory. Temperature-dependent time-resolved emission spectroscopy showed an increase of the acceptor emission lifetime with decreasing temperature. It also indicates the presence of different conformations because two different electron transfer barriers (0.08 and 0.42 eV) were found. These barrier values were corroborated by a theoretical analysis of the energetics of the process using Marcus theory, indicating average donor−acceptor distances of 4.5 Å (room temperature) to 11 Å (at low *T*).

Introduction

The supramolecular organization of chromophoric units into large photoactive assemblies constitutes one of the challenges for nanophotonics,[1−6] inspired by nature's photosynthetic reaction center.[7] For this aim, designed building blocks are needed that incorporate the right energetics for the antenna effect and the charge separation to display a combination of efficient energy and electron transfer events in multichromophoric structures, as in the cornerstone of natural photosynthesis. Next to these properties the building blocks should contain structural elements that can be used for further supramolecular construction to obtain a final system that is organized in space, energy, and time. The latter means that the photoinduced processes should be consecutive to obtain high energy and electron transfer yields. In nanophotonics these processes are of importance for the development of artificial devices for the conversion of light into chemical or electrical energy or vice versa.[8−11]

Although the study of photoinduced energy and electron transfer in bichromophoric and multichromophoric systems is a greatly developed field,[12−16] the design of efficient light harvesting systems combined with an electron donor−acceptor pair is more scarce.[17]

Especially during the last years several groups focused their attention on perylene bisimide dyes (both non-bay-substituted and bay-functionalized) as building blocks for photoactive systems.[18−37] These dyes are highly photostable and normally exhibit fluorescence quantum yields of almost unity[38,39] and an almost negligible triplet yield.[38] Accordingly, some undesired processes for the purpose described above, such as triplet state population and radiationless deactivation through vibrational relaxation are absent. Next to their very high ground state absorption coefficients, another favorable feature of these dyes is the well-defined absorbance of their radical anionic states[40,41] at about 800 nm that allows easy detection of electron transfer events[42] in the photoexcited state.

In this paper we describe the synthesis and photophysical properties of a model perylene system (**3**) and of a two-component system containing the same perylene bisimide acceptor and four pyrene moieties as donor (**2**) (Scheme 1). The understanding of their properties as well as the photoinduced processes are of great interest for the construction of more complex structures by means of coordination of the pyridine units to metal ions leading to molecular squares.[43] A quantitative analysis of the processes as well as their rates have been obtained using UV−vis absorption, steady state and time-resolved emission, femtosecond transient absorption, temperature-dependent time-resolved emission and theoretical analysis of the energetics of the processes. A very preliminary study of these systems has been reported,[44] but here an extensive spectroscopic study, which clarifies many of the properties of these interesting systems, is presented. In particular, we found that both energy and electron transfer processes occur in such systems. These observations open a new and interesting approach for the realization of artificial photosynthetic systems.

Results and Discussion

Synthesis. The pyrene−perylene bisimide system **2** was obtained from *N*,*N*′-bis(4-pyridyl)-1,6,7,12-tetrakis(4-hydroxy-

* Corresponding authors. E-mail: F.W., wuerthner@chemie.uni-wuerzburg.de; R.M.W., williams@science.uva.nl.
[†] Universiteit van Amsterdam.
[‡] Universität Würzburg.

10.1021/jp0372688 CCC: $27.50
Published on Web 02/24/2004

SCHEME 1: Synthesis of the Tetra-Pyrene−Perylene Bisimide Dye (2) Together with Reference Perylene Bisimide Compound 3[a]

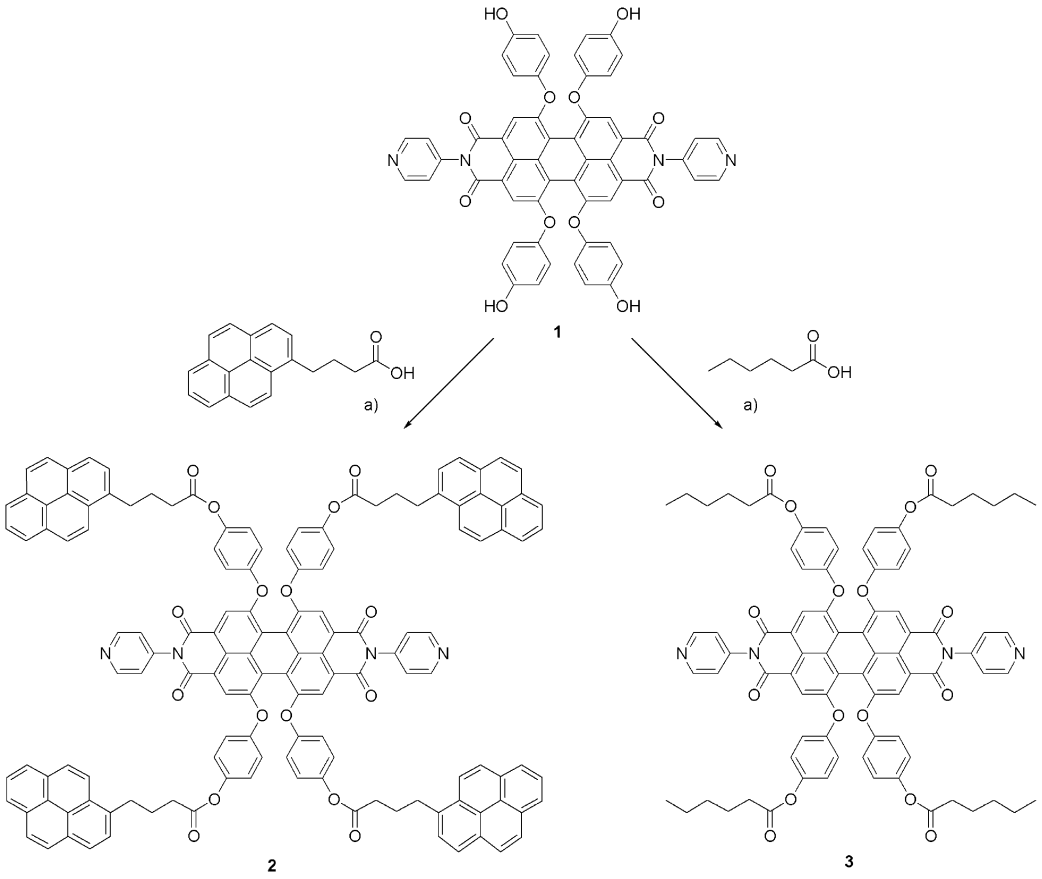

[a] DCC, DPTS, CH_2Cl_2, DMF, RT, 3d, 40−57%.

phenoxy)perylene-3,4,9,10-tetracarboxylic acid bisimide (**1**)[45] and pyrenebutyric acid by DCC/DPTS-promoted esterification according to the method of Moore and Stupp.[46,47] The reaction is carried out in dichloromethane at room temperature, and typically, yields higher than 90% per coupling step can be achieved.[46,47] Here, by reacting perylene bisimide **1** with pyrene butyric acid, the tetra-pyrene−perylene bisimide dye **2** was obtained in 40% yield after purification by chromatography. In the same way, reference compound **3** was obtained in 57% yield by reacting **1** with hexanoic acid (see Experimental Section for details). Thus, a relatively easy and flexible method for the synthesis of perylene based functional supramolecular building blocks is achieved.

Spectroscopy. *a. Steady State Spectroscopy.* Compounds **2** and **3** (Scheme 1) are dark purplish-black solids that, once dissolved homogeneously, display the typical bright pink-red color that is representative for tetraphenoxy-substituted perylene bisimides.

The UV−vis absorption spectra of the two compounds in dichloromethane are depicted in Figure 1, and the absorption data are summarized in Table 1. The absorption bands of the perylene unit give the characteristic $\pi-\pi^*$ transitions of the functionalized perylene bisimide[38,40] and match exactly for both compounds; 445 nm (belongs to S_0-S_2 electronic transition), 535 and 575 nm (belong to S_0-S_1 electronic transition).[48,49] The pyrene absorption bands of compound **2** dominate the UV region of the spectrum with five sharp characteristic pyrene transitions at 267, 278, 314, 328, and 344 nm. The distinct absorption patterns belonging to the pyrene and perylene units allow the virtually selective excitation of these chromophores present in compound **2**.

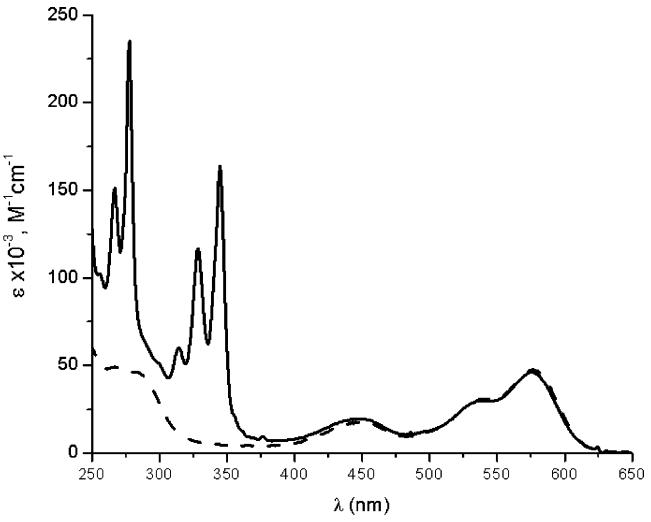

Figure 1. Absorption spectra of compound **2** (solid line, 1.93×10^{-6} M) and **3** (dashed line, 2.0×10^{-6} M) in dichloromethane.

The emission spectra of compound **2** and **3** in isoabsorptive dichloromethane solutions at room temperature were recorded upon excitation at 336 nm, where the pyrene units absorb strongly (see Figure 2). Both compounds have an emission maximum around 610 nm with a shoulder at 670 nm, typical of the perylene moiety.[39,48] For compound **2** containing two chromophores, i.e., the pyrene and the perylene units, an emission from the pyrene moiety between 380 and 460 nm could be expected. However, compound **2** displays strongly quenched pyrene emission in this wavelength region (vide infra) and a

TABLE 1: Summary of the Photophysical Properties of Compounds 2 and 3[a]

			emission at RT					
compounds	solvents	absorption λ (nm) (ϵ (M^{-1} cm^{-1}))	λ_{pyr} (nm)	λ_{per} (nm)	τ_{pyr} (ns)	τ_{per} (ns)[b]	Φ_{pyr}	Φ_{per}
2	toluene	330, 346, 448, 530, 570	377	601	0.28	3.9	0.0042	0.39
	DCM	328, 344 (162 300), 448, 538, 575 (45 800)	378	611	0.24	1.0	0.0011	0.12[c,d]
3	toluene	288, 448, 534, 572		602		6.0[c]		0.97
	DCM	283, 450, 539, 575 (47 300)		610		6.3[c]		0.90

[a] Excitation wavelengths are 324 nm for lifetimes unless otherwise indicated. [b] The following rise times were also observed for the perylene emission of compound **2**; 0.22, 0.21, in the two respective solvents. [c] $\lambda_{ex} = 336$ nm. [d] $\lambda_{ex} = 545$ nm.

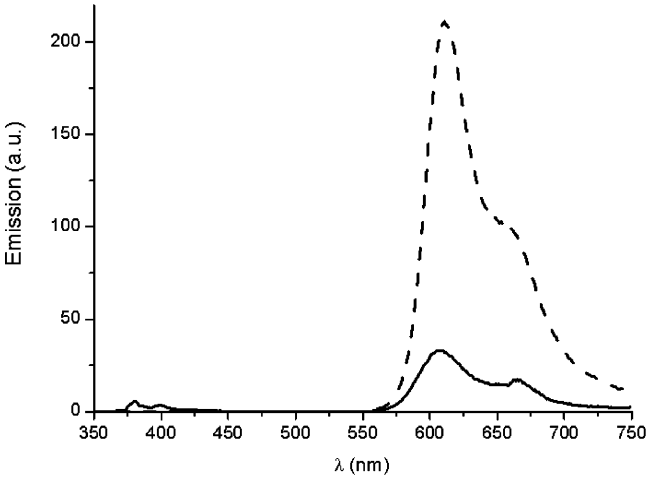

Figure 2. Emission spectra of compound **2** (solid line) and **3** (dashed line) in dichloromethane, $\lambda_{ex} = 336$ nm, spectra are corrected according to absorptions at 336 nm.

sensitized emission from the lower energy perylene chromophore is observed. If a photoinduced energy transfer is the only process present upon excitation of the pyrene unit, the emission quantum yield of the perylene unit should resemble that of the model compound **3**. As can be seen in Figure 2, however, also the emission intensity of the perylene unit of compound **2** is strongly quenched (~70%) as compared to the reference compound **3**. No additional emission or absorption bands were observed due to excimer and/or exciplex formation. The photophysical properties of **2** and **3** are summarized in Table 1.

The quantum yields of compound **2** were determined for both the pyrene and the perylene emission, by exciting the pyrene and the perylene units at the wavelengths indicated in Table 1. For the pyrene moiety, a strong quenching of the pyrene emission ($\Phi_f = 0.0011$ in dichloromethane) is observed as compared to the reference, pyrene itself, $\Phi_f = 0.65$ in nonpolar solvent.[50] As can be seen from the data summarized in Table 1, the emission quantum yields of the perylene unit are significantly lower when compared to the reference compound **3** ($\Phi_f = 0.90$ in dichloromethane). It is also found that the emission quantum yield of the perylene moiety is independent of the excitation wavelength and was determined to be 0.12 in dichloromethane. This indicates that independent of the excitation energy, the lowest excited state located on the perylene unit is populated. Only in toluene, which is a nonpolar solvent, a relatively higher perylene emission quantum yield ($\Phi_f = 0.39$) was observed. As can be clearly seen from the emission spectra depicted in Figure 2 and the quantum yield determinations, apart from the energy transfer, an additional process takes place that quenches the perylene emission. This process was investigated by further study with time-resolved techniques.

b. Time-Resolved Spectroscopy. Time-Resolved Emission Spectroscopy. As expected, the decay times of the pyrene emission, recorded at 400 nm, are similar in solvents of different polarity (see Table 1), in agreement with the solvent independence normally observed for Förster type energy transfer.[51] From the data shown in Figure 3, an accurate evaluation of the rate of photoinduced energy transfer is obtained. Upon excitation of the pyrene unit, quenching of the pyrene and a rise time on the perylene moiety is observed (see Figure 3, left). The sensitized perylene unit decays with a shorter lifetime than the reference compound **3** (Figure 3, right). The reference compound **3** shows a monoexponential decay, and no rise time.

The rise time of compound **2**, which has a similar value in both solvents, represents the formation of the excited state of the perylene unit by energy transfer from the pyrene excited state and the decay time is due to the quenched emission of the perylene unit. Such quenching indicates that an additional process takes place while energy is transferred to the perylene

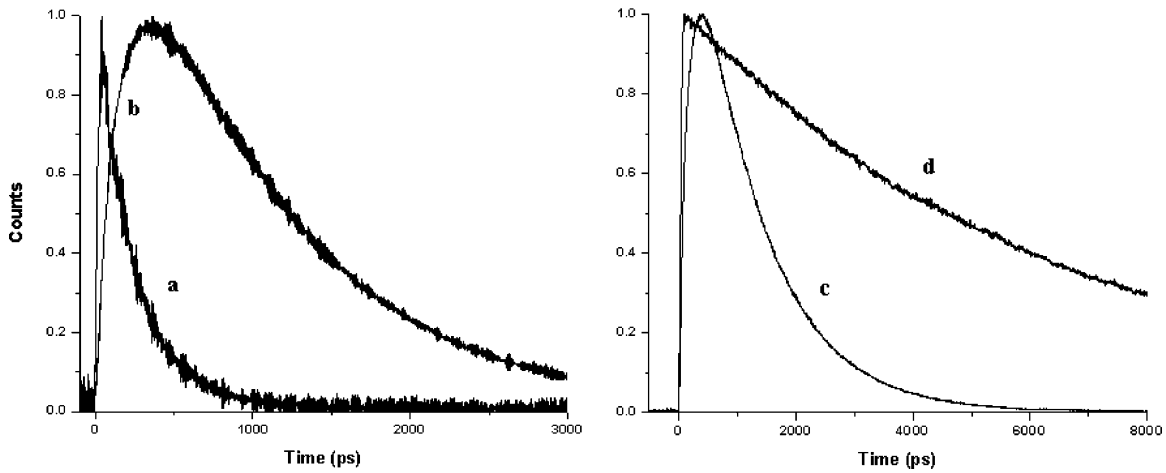

Figure 3. Time-resolved emission traces of compound **2** and **3** in dichloromethane (measured with single photon counting, $\lambda_{ex} = 324$ nm): quenched lifetime of the pyrene moiety of **2** measured at 400 nm (a); the rise time of the perylene unit of **2** at 650 nm (b); quenched emission of the perylene unit of **2** at 650 nm (c); emission of compound **3** at 650 nm (d). All traces are deconvoluted signals.

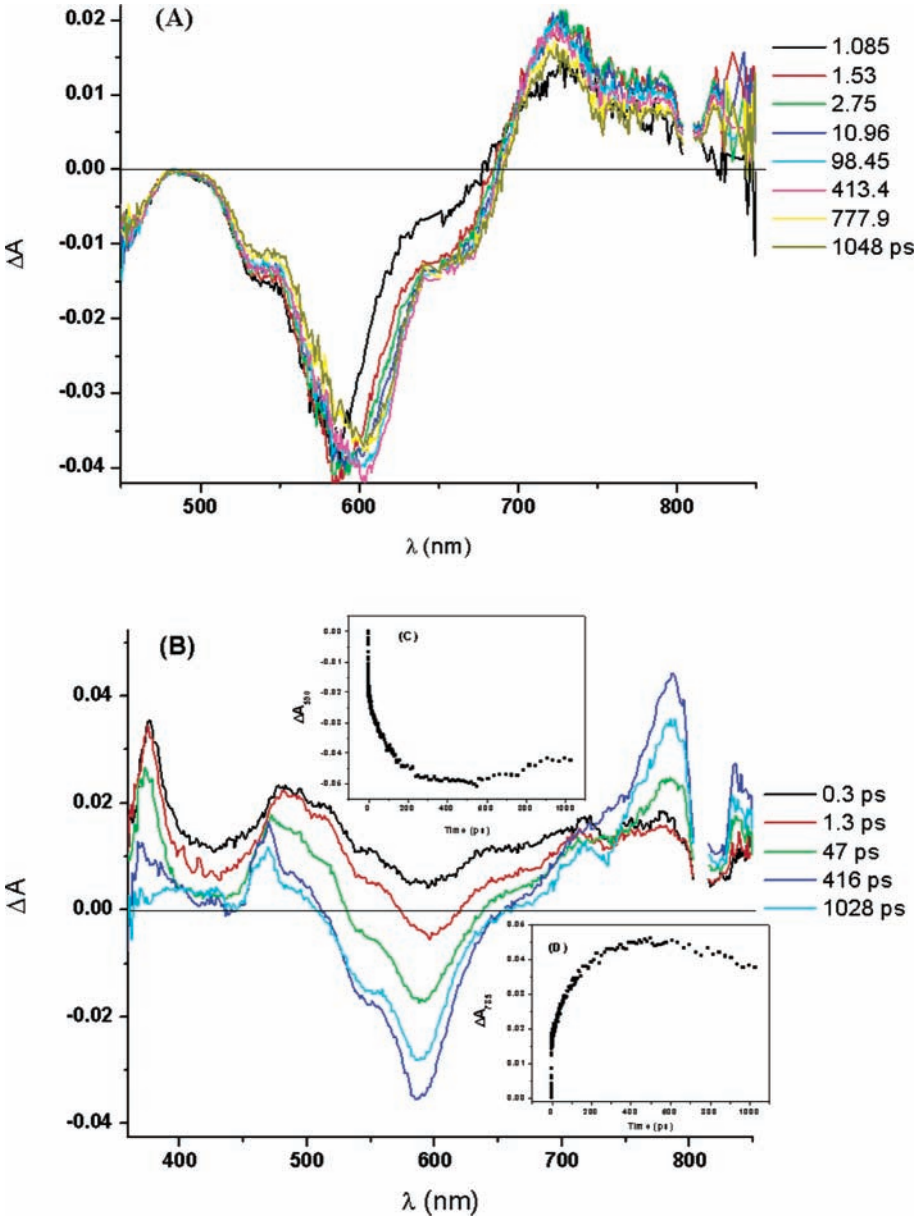

Figure 4. Femtosecond transient spectra of compounds **3** (above, A) and **2** (below, B) in dichloromethane. Time delays corresponding to frames are written in the spectra (λ_{ex} = 345 nm, 130 fs fwhm). (C) Kinetic profile of the transient absorption determined at 590 nm. (D) Kinetic profile of the transient absorption determined at 785 nm.

unit. It is well-known that pyrene and perylene units are good donor and acceptor groups, respectively; therefore it is not surprising that an electron transfer occurs from the excited perylene (vide infra). The different photophysical behavior in toluene also supports the occurrence of an electron transfer that is less efficient in such a nonpolar medium. These experiments indicate that the charge-separated state is less populated in toluene due to the less efficient (endergonic) electron transfer.

The energy transfer process is visualized in Figure 3. As can clearly be noted, the rise time measured for the perylene emission (0.21 ns) is almost identical to the decay of the quenched pyrene emission (0.24 ns) in dichloromethane. This allows the calculation of the rate following the equation [$k_{en} = 1/\tau - 1/\tau_{ref}$], giving $k_{en} \approx 4.2 \times 10^9$ s^{-1} for compound **2** (τ_{ref} = 650 ns[50]).

As the emission results indicate the presence of a charge-separated state, nanosecond transient absorption in dichloromethane was performed with compound **2**. The aim was to observe the formation of the transient species as a consequence of photoinduced charge separation. However, it was observed that this process is faster than the response time of the nanosecond equipment (ca. 1−2 ns).

Femtosecond Transient Absorption Spectroscopy. By using femtosecond time-resolved spectroscopic techniques, insight has been gained into the excited state properties responsible for the photoinduced behavior of compounds **2** and **3** in dichloromethane. The femtosecond transient absorption spectra of compounds **2** and **3** and kinetics belonging to **2** in dichloromethane are depicted in Figures 4 and 5.

In the reference compound **3**, the transient absorption spectra show an intense bleaching at 590 nm and a strong $S_1 \rightarrow S_n$ perylene excited state transition centered at 725 nm. In this time scale no recovery of the ground state was observed because, as previously mentioned, the excited state lifetime is in the nanosecond time regime.

The femtosecond transient absorption spectra of compound **2** contain a wealth of information in which the singlet singlet absorption ($S_1 \rightarrow S_n$) of the pyrene (at 482 and 514 nm), the

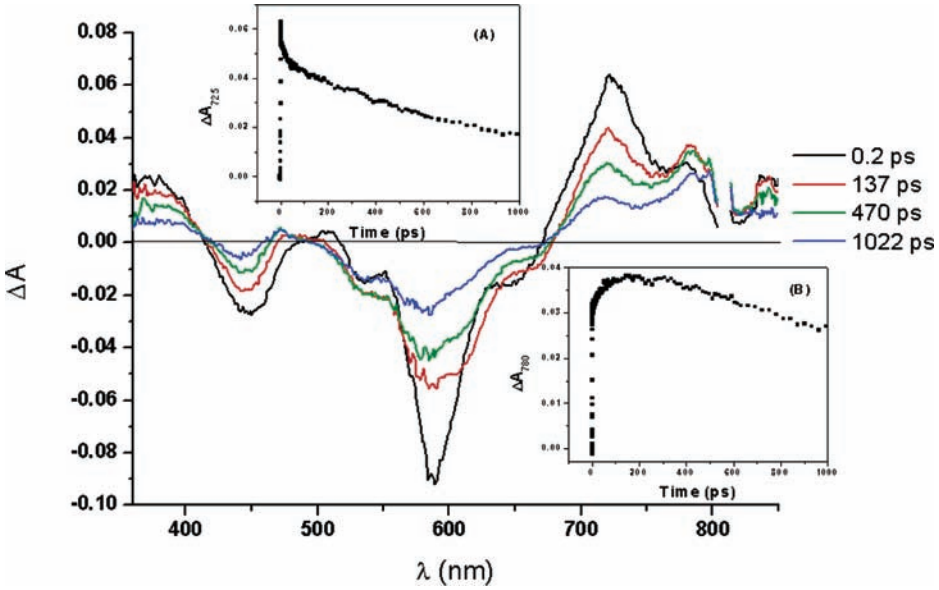

Figure 5. Femtosecond transient spectrum of compound **2** in dichloromethane, time delays corresponding to frames are written in the spectra (λ_{ex} = 575 nm, 130 fs fwhm). Kinetic profiles of the transient absorbance of compound **2** determined at 725 (A) and 780 nm (B) in dichloromethane.

radical cation of the pyrene (around 470 nm),[52] the ground state bleaching of the perylene (between 500 and 650 nm), and the radical anion of the perylene (around 800 nm)[40,43] can be observed. Comparison with model compound **3** clearly indicates that the charge-separated state consisting of the radical anion of acceptor and the radical cation of the donor is formed within 200 ps. The spectroelectrochemistry performed on a similar bay-functionalized perylene bisimide[43] confirms the 700−800 nm band of the radical anion of the perylene. Femtosecond transient absorption spectra obtained by excitation at 345 and 575 nm were recorded. Kinetic profiles of the transient of compound **2** were probed at 590 and 785 nm in the case of λ_{ex} = 345 nm, and 725 and 780 nm upon excitation at 575 nm.

As discussed earlier, excitation at 345 nm could lead to energy and/or electron transfer processes. As can be seen in Figure 4b, after excitation at 345 nm, first the absorption of the $S_1 \rightarrow S_n$ transition of the pyrene excited state was observed[53] in the first picoseconds with maxima at 482 and 514 nm. Subsequently, the energy transfer process can be observed from pyrene moieties to the perylene unit because the bleaching of the perylene moiety around 590 nm indicates the formation of the excited state of the perylene. The pyrene radical cation is formed at 470 nm with a shoulder at 489 nm. According to the kinetic profile at 519 nm (data not shown here), the pyrene singlet excited state decays in 0.13 ns corresponding to the 0.12 ns rise time at 590 nm (ground state bleaching, Figure 4b, inset C). This kinetics is very much in line with the decay measured by the time-resolved emission spectra. On the similar time scale of the energy transfer process, an efficient electron transfer is observed, as shown by the formation of the radical anion at 785 nm and the radical cation at 470 nm. Analysis of the kinetics at 785 nm gives a 0.16 ns rise time (Figure 4b, inset D) followed by a longer decay time (1.7 ns). A similar long component was observed at 590 nm (1.4 ns) and it is assigned to the decay to the ground state. As can be understood from these values, the energy and electron transfers have almost the same rates.

In the case of excitation of compound **2** at 575 nm, where only the perylene moiety absorbs, energy transfer cannot be observed. Excitation causes the formation of both the strong absorption at 725 nm due to the $S_1 \rightarrow S_n$ transition of the perylene bisimide and the bleaching at ∼580−590 nm due to the depopulation of the ground state (Figure 5). The spectral

TABLE 2: Summary and Comparison of the Rise and Decay Times of 2 in Dichloromethane with Two Techniques[a]

	time-resolved emission spectroscopy[b]		femtosecond transient spectroscopy			
λ_{det} (nm)	400	650	590[c]	785[c]	725[d]	781[d]
τ_{rise} (ns)		0.20	0.12	0.16		0.078
τ_{decay} (ns)	0.24	1.0	1.4	1.7	0.90	2.1

[a] All data were recorded in dichloromethane. [b] λ_{ex} = 324 nm. [c] λ_{ex} = 345 nm. [d] λ_{ex} = 575 nm. According to the data recorded at 590 and 725 nm, also very fast components were observed of 3.5 and 7 ps, respectively for compound **2**.

changes indicate the formation of the radical anion of the perylene bisimide and the radical cation of pyrene that are formed within 70 ps after excitation. The kinetic profile at 725 nm (Figure 5, inset A) results in monoexponential decay with a value of 0.900 ns due to the back electron transfer to reestablish the ground state. Kinetic data obtained according to the 472 (data not shown) and 780 (Figure 5, inset B) nm transients give 0.070 and 0.078 ns rise times corresponding to the radical cation and anion formations, respectively. As can be seen from the kinetic traces at 780 nm in Figure 5, inset B, the formed charge-separated species decays on the longer time scale. A summary of the decay times for compound **2** is provided in Table 2. Kinetic results at 590 and 720 nm showed additional very fast components, ∼3.5 and 7 ps, which can be attributed to the vibrational/solvent relaxation according to literature discussions.[36,54]

Comparison between the transient absorption spectra recorded at the two different excitation wavelengths suggests the following conclusion: At 345 nm, the first observed process is the excitation of the pyrene followed by an efficient energy transfer to the perylene moiety. However, the population of the excited state of the perylene, reflected in its singlet−singlet absorption at 725 nm, is much lower than expected (see spectra recorded at 575 nm excitation), because an electron transfer occurs at the same time scale as the energy transfer.

It is interesting to notice that no (faster) direct electron transfer from the excited pyrene to the perylene acceptor is observed. Electron transfer occurs after energy transfer, leading to population of the perylene singlet excited state. The reason for the absence of a direct photoinduced electron transfer could be

SCHEME 2: Energy Level Diagram of Compound 2 in Dichloromethane Showing Energy and Electron Transfer Pathways, upon Excitation of the Pyrene (Left) and of the Perylene (Right) Units[a]

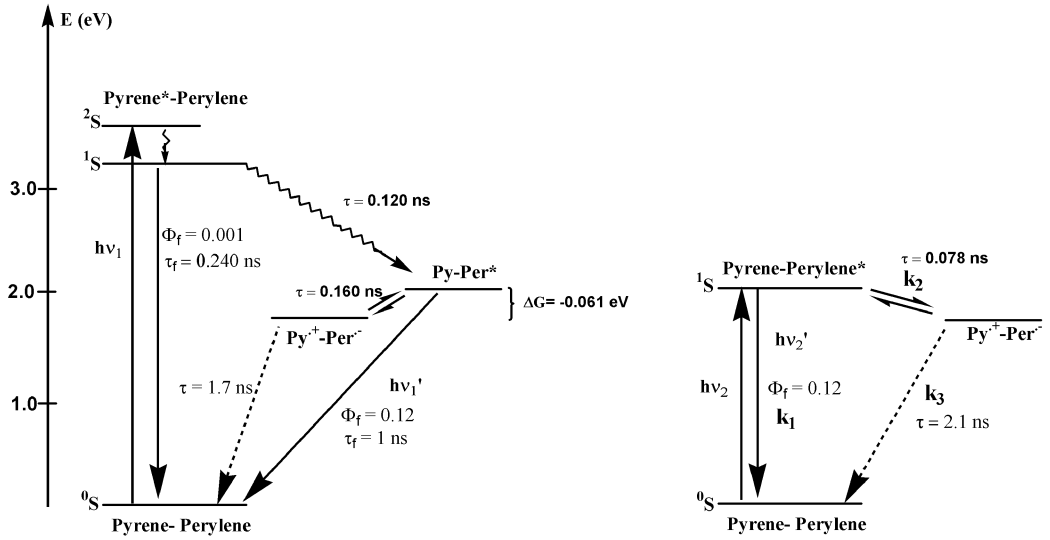

[a] All τ values are experimentally observed results in the scheme; see text for further information.

the extremely exergonic process ($\Delta G = -1.38$ eV, $\lambda = 0.44$ eV, $\Delta G^{\#} = 0.51$ eV) that results in a slow electron transfer process because it falls in the Marcus inverted region.[60]

The processes occurring upon excitation of **2** with either visible or UV light are depicted in the energy diagram in Scheme 2.

The rates observed for the energy transfer process obtained with transient spectra and time-resolved emission experiments are very close to each other ($k_{en} = 8.3 \times 10^9$ s^{-1}, $k_{en} = 4.2 \times 10^9$ s^{-1}, respectively). On the contrary, there is a clear difference between the apparent rates obtained for the electron transfer process. With time-resolved emission, rates are obtained of 8.4×10^8 s^{-1}, and transient absorption indicates an experimental rate of formation of the charge transfer state of 6.6×10^9 s^{-1} (from 345 nm excitation).

The difference in apparent rates must be attributed to a delayed luminescence from the perylene singlet excited state, which is in equilibrium with the charge transfer state. Because of the presence of such equilibrium, the charge-separated state decay time and the fluorescent lifetime of the perylene moiety have a similar value (1.0−2.0 ns). The charge-separated state indeed lies at energy levels comparable with the singlet excited state of the perylene (see Scheme 2). Therefore, equilibrium between the two states is observed that is responsible for the observed rate of the two processes.

The individual rate constants in case of excitation of the perylene moiety can be calculated using the kinetic model outlined in Scheme 2. The model is represented by the following system of equations:

$$\frac{1}{2}\left(k_1 + k_2 + k_{2'} + k_3 + \sqrt{(k_1 + k_2 - k_3 - k_{2'})^2 + 4k_2k_{2'}}\right) = \kappa_1$$

$$\frac{1}{2}\left(k_1 + k_2 + k_{2'} + k_3 - \sqrt{(k_1 + k_2 - k_3 - k_{2'})^2 + 4k_2k_{2'}}\right) = \kappa_2$$

$$k_1 = \frac{1}{6.3 \times 10^{-9}}$$

$$\frac{k_2}{k_{2'}} = 11$$

TABLE 3: Acceptor Lifetime at 650 nm and Rates of Charge Separation in Dichloromethane, Together with λ, ΔG_{cs}, and $\Delta G^{\#}$ at Various Temperatures

	experimental		calculated		
T (K)	τ (ns) at 650 nm	k_{cs} (10^8 s^{-1})	ΔG_{cs} (eV)	λ (eV)	$\Delta G^{\#}$ (eV)
295	1.05	7.94	−0.061	0.436	0.081
281	1.22	6.58	−0.064	0.437	0.080
270	1.34	5.88	−0.066	0.438	0.079
263	1.40	5.53	−0.067	0.439	0.079
252	1.62	4.57	−0.069	0.440	0.078
242	1.81	3.85	−0.071	0.441	0.077
232	1.91	3.57	−0.073	0.441	0.077
222	2.06	3.19	−0.075	0.442	0.076
212	2.32	2.65	−0.077	0.443	0.076
202	2.90	1.74	0.054	1.593	0.426
193	4.22	0.67	0.045	1.596	0.422
182	5.52	0.12	0.036	1.598	0.418

[a] The temperature dependence of dielectric constant and refractive index were calculated according to following equations:[63] $\epsilon(T) = 40.452 + T(0.00023942T - 0.17748)$ and $n(T) = 1.4244 - 0.000562(T - 293)$. $R_{c1-9} = 4.5$ Å, $R_{c10-12} = 11$ Å, $r = 4$ Å, $\lambda_i = 0.2$ eV, $E_{ox} = 1.6$ V vs SCE, $E_{red} = -0.49$ V vs SCE, $E_{00} = 2.1$ eV.

where κ_1 and κ_2 are the experimentally observed rate constants. Because it is not possible to obtain four constants from the biexponential fit, the value of k_1 was taken from the fluorescence decay rate of the model compound (**3**). The equilibrium constant $k_2/k_{2'}$ was calculated from $\Delta G = -RT \ln K_{eq}$ using $\Delta G = -0.061$ eV (see next section, Table 3) at $T = 295$ K. The solution of the equations yields the individual rate constants $k_1 = 1.59 \times 10^8$ s^{-1}, $k_2 = 1.16 \times 10^{10}$ s^{-1}, $k_{2'} = 1.05 \times 10^9$ s^{-1}, and $k_3 = 5.06 \times 10^8$ s^{-1}. As the results clearly suggest, there is an equilibrium established between the charge-separated state and the singlet excited state of the perylene bisimide. Note that k_2 and $k_{2'}$ are the forward and backward rate for the equilibrated states, respectively.

By using the experimentally obtained energy transfer rate, an effective interaction radius between donor and acceptor groups can be calculated.[55]

The rate of energy transfer depends on the extent of spectral overlap of the emission spectrum of the donor with the absorption spectrum of the acceptor, the quantum yield of the donor, the relative orientation of the donor and acceptor

transition dipoles, and the distance between the donor and acceptor molecules.[56] Because we think that there is a Förster type energy transfer, the distance between donor (D) and acceptor (A) plays an important role. The distance at which energy transfer is 50% efficient, called the Förster distance, is typically in the range of 20−60 Å. The rate of energy transfer from a donor to acceptor is given by

$$k_{en} = (R_0/R)^6 k_D \quad (1)$$

and

$$k_D = 1/\tau_D \quad (2)$$

where τ_D is the decay of the donor in the absence of acceptor, R_0 is the Förster distance, R is the donor-to-acceptor distance. Any change in D−A distance will affect the energy transfer rate. Because of this fact, energy transfer measurements have been used to estimate the distances between sites on macromolecules and the effects of conformational changes on these distances.[55,57]

To calculate the Förster distance, R_0, the following simplified equation can be used

$$R_0 = 0.211[\kappa^2 n^{-4} \Phi_D J(\lambda)]^{1/6} \quad (3)$$

where κ^2 is the orientation factor, and generally assumed as $^2/_3$ in calculations, n is the refractive index of the medium, Φ_D is the quantum yield of the donor in the absence of acceptor, and $J(\lambda)$ is the overlap integral of the donor emission and the acceptor absorption. Once R_0 is calculated from these experimentally known values, the distance between donor and acceptor can be easily obtained.

From our experimental values, R_0 is calculated using eq 3 as 34.3 Å, where, $\kappa^2 = {}^2/_3$, $n_{DCM} = 1.4240$, $\Phi_D = 0.65$, and $J = 1.75 \times 10^{14}$ M^{-1} cm^{-1} nm^4. It should be noted that because the emission of the pyrene group attached to the perylene moiety has a rather noisy signal, for the spectral overlap, $J(\lambda)$, the emission spectrum of the pyrene itself was used. It was found that the $J(\lambda)$ value did not change significantly.

Knowing the values of τ_D as 650 ns, the energy transfer rate as 6.2×10^9 s^{-1}, and R_0, the donor−acceptor distance (R) can be calculated by using eqs 1 and 2. This leads to a value of 8.6 Å.

c. Temperature-Dependent Time-Resolved Emission Spectroscopy. Having established the photoinduced processes in compound **2**, we decided to study the temperature dependence of the lifetime of the perylene bisimide acceptor unit with time-resolved emission spectroscopy. The aim is to gain information on the energetics of the system and to determine the barrier for the photoinduced electron transfer process experimentally.

The excited state lifetimes of compound **2** have been measured at temperatures in the range between 295 and 182 K and were analyzed using a modified Arrhenius plot (see Figure 6). From the slope of $\ln(k_{cs}T^{0.5})$ vs $1/T$, the value of $\Delta G^{\#}$ can be estimated.[58] The lifetime of the compound **3** was used as a reference, and its lifetime upon temperature change was taken into account in dichloromethane (6.3 ns around room temperature and 5.9 ns at the lowest temperature).

All the data are summarized in Table 3, in which τ is the lifetime of the perylene emission obtained from the decay at 650 nm after excitation at 324 nm, and k_{cs} is the rate constant calculated according to eq 5 (see Experimental Section) when compound **3** was used as reference. λ, ΔG_{cs}, and $\Delta G^{\#}$ are calculated by using the Marcus model.[59,60]

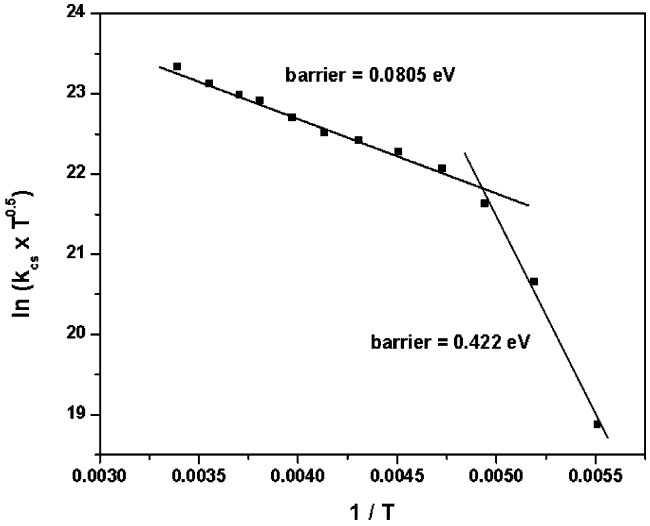

Figure 6. Modified Arrhenius plot for photoinduced charge separation of **2** in dichloromethane, with two barrier values.

In Table 3 the change of the lifetime of the perylene emission with temperature can be observed, and it approaches the value of the reference system at around 180 K.

Furthermore, the deduced electron transfer rates are presented. With these rates the modified Arrhenius plot is constructed, and it clearly shows two temperature regions, where a different behavior is found (see Figure 6). The data were fitted using two series of data, between room temperature and 212 K, and between 202 and 182 K. These fits result in two barrier values. The lower barrier value (0.08 eV) is most representative as the time-resolved studies were performed at room temperature, whereas a barrier of 0.42 eV was obtained for the lower temperatures range. An intercept of 26.5 (=ln k_{opt}) was obtained.

On the right side of Table 3, calculated values for the driving force (ΔG_{cs}), the reorganization energy (λ), and the barrier to electron transfer ($\Delta G^{\#}$) are presented, using the standard Rehm−Weller approach, in combination with the Marcus model. Under Table 3, the redox data, singlet state energy (E_{00}), and temperature correction for n and ϵ are described. Good agreement between the calculated and experimentally observed barriers to electron transfer was obtained by adjusting the center-to-center distance (R_c) between the two chromophores in the barrier calculation. As indicated, an R_c value of 4.5 Å was used for the first 9 data points (the high-temperature region), and a value of 11 Å for the last three data points (the low-temperature data set).

This analysis thus allows for an interpretation of the two barriers, relating them to two possible conformations of compound **2**. These two conformations can be (i) a folded one with an average center-to-center (R_c) distance between the pyrene and perylene groups of about 4.5 Å and (ii) a stretched conformer with $R_c = 11$ Å at low temperature.

It is found that the barrier is temperature dependent and this could be related to conformational changes of the compound as the temperature is lowered; i.e., at low temperature a smaller number of conformations is present, which have on average a larger interchromophore distance than at room temperature.

The temperature dependence of the pyrene emission was also monitored over the same temperature trajectory and was found to be virtually temperature independent. The lifetime ranges from 256 ps at room temperature to 370 ps at the lowest temperature. The barrier for energy transfer obtained from the (linear) modified Arrhenius plot is calculated to be 0.03 eV.

This is in agreement with the temperature behavior of Förster type energy transfer.[51]

Conclusions

The photophysical properties of a building block that can be used in metallosupramolecular architectures, like squares, triangles, and other assemblies, have been established. Fast photoinduced energy transfer ($k_{en} \approx 6.2 \times 10^9$ s^{-1}, average value) with a high yield (>90%) is followed by efficient electron transfer (70%, $k_{et} \approx 6.6 \times 10^9$ s^{-1}). Both processes occur from the pyrene unit to the perylene moiety. Picosecond-resolved emission and transient absorption spectroscopy give clear evidences for the occurrence of these two processes.

Determination of the barrier to electron transfer yields a relatively low value of 0.08 eV at room temperature, but a higher barrier of 0.42 eV is observed in a lower temperature trajectory. This behavior can be explained by assuming two possible conformations, in which the center-to-center distance ranges from 4.5 to 11 Å. The latter is preferred at low temperature and is in accordance with a more stretched conformation.

Whereas the temperature dependence indicates the presence of more conformations, the time-resolved studies at room temperature give an image of an average conformation, without components attributable to individual (stretched or folded) conformations.

The time-resolved and steady state emission gives clear proof of energy transfer from the pyrene to the perylene bisimide. The Förster distance is calculated to be 34.3 Å and the corresponding donor−acceptor distance is calculated from the energy transfer rate as 8.6 Å. No indications for energy hopping between different pyrene moieties are observed. Furthermore, the femtosecond transient absorption data do not give an indication of very fast, direct electron transfer (circumventing the energy transfer to the perylene unit), due to Marcus inverted region effects ($\Delta G = -1.38$ eV, $\lambda = 0.44$ eV, $\Delta G^{\#} = 0.51$ eV). Clearly, a direct photoinduced electron transfer upon pyrene excitation ($E_{00} = 3.42$ eV) is not fast enough to compete with energy transfer due to a high electron transfer barrier.

Thus a functional photoactive building block has been obtained that displays two processes, energy transfer and electron transfer, and the effects of supramolecular organization on these processes can now be pursued.

Experimental Section

Synthesis. Solvents and reagents were purchased from Merck (Darmstadt, Germany) unless otherwise stated and purified and dried according to standard procedures.[61] Column chromatography was performed on silica gel (Merck Silica 60, particle size 0.063−0.2 mm) and on a Merck-Lobar-C (LiChroprep Si60) column. 4-(Dimethylamino)pyridinium-4-toluenesulfonate (DPTS)[47] has been synthesized according to the literature. ^{1}H NMR spectra were recorded on a Bruker DRX 400 or AMX 500 spectrometer using TMS as internal standard. MALDI-TOF spectra were recorded on a Bruker-Franzen Reflex III spectrometer. The calculated and found *m*/*z* values correspond to the monoisotopic masses.

***N,N′*-Bis(4-pyridyl)-1,6,7,12-tetrakis{4-[(4-pyren-1-ylbutanoyl)oxy]phenoxy}perylene-3,4:9,10-tetracarboxylic Acid Bisimide (2).** *N,N′*-Bis(4-pyridyl)-1,6,7,12-tetrakis(4-hydroxyphenoxy)perylene-3,4:9,10-tetracarboxylic acid bisimide **1** (51.5 mg, 0.048 mmol; **1**·6H_2O) and 4-pyren-1-ylbutyric acid (93.0 mg, 0.322 mmol) were dissolved in a mixture of DMF (2.5 mL)/CH_2Cl_2 (5 mL), and DPTS (104.3 mg, 0.354 mmol) and dicyclohexylcarbodiimide (DCC) (83 mg, 0.403 mmol) were added under argon. After stirring for 2.5 h at room temperature, additional DCC (100 mg) was added and stirring was continued for 20 h. After addition of CH_2Cl_2 (20 mL) the mixture was filtered and the solution was concentrated (ca. 2 mL). Precipitation with methanol and thorough washing with methanol afforded the crude product **2**, which was purified by chromatography on a Merck-Lobar-C (LiChroprep Si60) column (CH_2Cl_2/MeOH 98:2).

Yield: 40 mg (40%) of **2**. Mp: >300 °C. ^{1}H NMR (400 MHz, $CDCl_3$, 25 °C, TMS): $\delta = 8.78$ (d, ^3J(H,H) = 6.1 Hz, 4H; $H_{\alpha-py}$), 8.26 (s, 4H; H_{per}), 8.23 (d, ^3J(H,H) = 9.3 Hz, 4H; $H_{pyr,9}$), 8.14−8.10 (m, 8H; $H_{pyr,5,7}$), 8.043 (d, ^3J(H,H) = 9.6 Hz, 4H; $H_{pyr,8}$), 8.041 (d, ^3J(H,H) = 7.6 Hz, 4H; $H_{pyr,2}$), 7.98 (m, 8H; $H_{pyr,3,4}$), 7.95 (t, ^3J(H,H) = 7.6 Hz, 4H; $H_{pyr,6}$), 7.78 (d, ^3J(H,H) = 7.7 Hz, 4H; $H_{pyr,1}$), 7.25 + $CHCl_3$ (d, 4H; $H_{\beta-py}$), 7.02 (d, ^3J(H,H) = 9.1 Hz, 8H; H_{ar}), 6.90 (d, ^3J(H,H) = 9.1 Hz, 8H; H_{ar}), 3.35 (t, 8H; H_{CH_2}), 2.60 (t, 8H; H_{CH_2}), 2.20 (m, 8H; H_{CH_2}). UV−vis (CH_2Cl_2): λ_{max} (ϵ) = 575 (45 800), 538 (29 400), 448 (18 400), 344 (160 400), 328 (116 100), 314 (57 800), 277 (216 600), 266 nm (143 100 mol^{-1} dm^3 cm^{-1}). MS (MALDI-TOF, dithranol) calcd 2056.6 *m*/*z*; found 2057.1 *m*/*z*. Elemental analysis: calcd (%) for $C_{132}H_{88}N_4O_{16}$ (2058.2) C 80.53, H 4.31, N 2.72; found C 79.98, H 4.34, N 2.61.

***N,N′*-Bis(4-pyridyl)-1,6,7,12-tetrakis[4-(hexanoyloxy)phenoxy]perylene-3,4:9,10-tetracarboxylic Acid Bisimide (3).** *N,N′*-Bis(4-pyridyl)-1,6,7,12-tetrakis(4-hydroxyphenoxy)perylene-3,4:9,10-tetracarboxylic acid bisimide **1** (45 mg, 0.042 mmol; **1**·6H_2O), hexanoic acid (Fluka, 58 μL, 0.46 mmol), and DPTS (135 mg, 0.46 mmol) were suspended in CH_2Cl_2 (10 mL) and dicyclohexylcarbodiimide (DCC) (95 mg, 0.46 mmol) and 4 drops of DMF were added under argon. After stirring for 3 days at 35 °C the reaction was worked up in the same way as described for **2** to give 33 mg (57%) of **3**.

Mp: >300 °C. ^{1}H NMR (400 MHz, $CDCl_3$, 25 °C, TMS): $\delta = 8.77$ (d, ^3J(H,H) = 6.0 Hz, 4H; $H_{\alpha-py}$), 8.20 (s, 4H_{per}), 7.24 (d, ^3J(H,H) = 6.0 Hz, 4H; $H_{\beta-py}$), 7.02 (d, ^3J(H,H) = 9.0 Hz, 8H; H_{ar}), 6.89 (d, ^3J(H,H) = 9.0 Hz, 8H; H_{ar}), 2.54 (t, 8H; H_{CH_2}), 1.75 (m, 8H; H_{CH_2}), 1.39 (m, 16H; H_{CH_2}), 0.94 (t, 12H, H_{CH_3}). UV−vis (CH_2Cl_2): λ_{max} (ϵ) = 575 (47 300), 538 (30 300), 448 (17 900), 282 (47 900), 269 nm (47 800 mol^{-1} dm^3 cm^{-1}). MS (MALDI-TOF, dithranol) calcd 1368.5 *m*/*z*; found 1368.3 *m*/*z*. Elemental analysis: calcd (%) for $C_{82}H_{72}N_4O_{16}$ (1369.5) C 71.92, H 5.30, N 4.09; found C 71.71, H 5.30, N 4.07.

Equipment and Procedures for the Determination of the Spectroscopic, Photophysical Properties. Electronic absorption spectra were recorded on a Hewlett-Packard UV−vis, diode array 8453 spectrophotometer. Steady state emission spectra were obtained from SPEX 1681 Fluorolog spectrofluorometer equipped with two double monochromators (excitation and emission) and are corrected for the photomultiplier response. Quantum yields of compounds were measured with respect to *N,N′*-bis(2,5-di-*tert*-butylphenyl)-3,4,9,10-perylenebis(dicarboximide) (DBPI) (0.98 in acetonitrile)[40] and *N,N′*-bis(2,6-diisopropylphenyl)-1,6,7,12-tetraphenoxyperylene-3,4:9,10-tetracarboxylic acid bisimide (0.96 in chloroform)[48] for the perylene emission in toluene and dichloromethane solutions, respectively. For the pyrene emission, anthracene (0.27 in ethanol)[62] was used as a reference in optically diluted solutions.

Both solvents used are spectroscopic grade and purchased from Acros and Merck Uvasol and distilled when it was necessary.

Time-resolved fluorescence measurements were performed on a picosecond single photon counting (SPC) setup. The

frequency doubled (300−340 nm, 1 ps, 3.8 MHz) output of a cavity dumped DCM dye laser (Coherent model 700) pumped by a mode-locked Ar-ion laser (Coherent 486 AS Mode Locker, Coherent Innova 200 laser) was used as the excitation source. A (Hamamatsu R3809) microchannel plate photomultiplier was used as detector. The instrument response (∼17 ps fwhm) was recorded using the Raman scattering of a doubly deionized water sample. Time windows (4000 channels) of 5 ns (1.25 ps/channel) to 50 ns (12.5 ps/channel) could be used, enabling the measurement of decay times of 5 ps to 40 ns. The recorded traces were deconvoluted with the system response and fitted to an exponential function using the Fluofit (PicoQuant) windows program.

For the low-temperature lifetime measurements an Oxford Instruments liquid nitrogen cryostat (DN704) was used in combination with picosecond single photon counting (SPC) setup.

In femtosecond transient absorption measurements, a Spectra-Physics Hurricane titanium:sapphire regenerative amplifier system was used as the laser system. The full spectrum setup was based on an optical parametric amplifier (Spectra-Physics OPA 800) as a pump. The residual fundamental light, from the pump OPA, was used for white light generation, which was detected with a CCD spectrograph. The OPA was used to generate excitation pulses at 345 and 575 nm. The laser output was typically 5 μJ pulse^{-1} (130 fs fwhm) with a repetition rate of 1 kHz. A circular cuvette (d = 1.8 cm, 1 mm, Hellma), with the sample solution, was placed in a homemade rotating ball bearing (1000 rpm), to avoid local heating by the laser beam. The solutions of the samples were prepared to have an optical density at the excitation wavelength of ca. 0.5 in a 1 mm cell. The absorbance spectra of the solutions were measured before and after the experiments, to check for degradation.

All photophysical properties reported here have an error bar of 5−10%. Measurements were mainly performed on aerated solutions. In some cases deaeration was applied, but no changes in behavior were found.

The energy barrier for electron transfer can be estimated experimentally in dichloromethane for compound **2**. According to the classical Marcus theory the rate of electron transfer can be described by

$$k_{et} = k_{opt} \exp[-(\lambda + \Delta G)^2/4\lambda k_B T] = k_{opt} \exp[-\Delta G^{\#}/k_B T] \quad (4)$$

where

$$k_{opt} = (2\pi^{3/2}/h(\lambda k_B T)^{1/2}) H_{rp}^{\ 2}$$

where h is the Plank constant, λ is the total reorganization energy, k_B is the Boltzmann constant, T is the temperature, and $\Delta G^{\#}$ is the electron transfer barrier.

The electron transfer barrier is calculated from the slope of modified Arrhenius type plot ($\ln(k_{cs}T^{0.5})$ vs $1/T$). The rate constant for charge separation, k_{cs}, is

$$k_{cs} = 1/\tau - 1/\tau_{ref} \quad (5)$$

Acknowledgment. Financial support from the DPI (Dutch Polymer Institute) for M.Z., from NWO (Nederlandse organisatie voor Wetenschappelijk Onderzoek) for the femtosecond equipment and from the UvA (Universiteit van Amsterdam) for B.K.K., L.D.C. AND R.M.W.) is gratefully acknowledged.

References and Notes

(1) Balzani, V. *Tetrahedron* **1992**, 10443−10514.
(2) *Electron Transfer in Chemistry*; Balzani, V., Ed.; Wiley-VCH: New York, 2001; Vols. 1−5.
(3) Barigelletti, F.; Flamigni, L. *Chem. Soc. Rev.* **2000**, *28*, 1.
(4) Scandola, F.; Indelli, M. T.; Chiorboli, C.; Bignozzi, C. A. *Top. Curr. Chem.* **1990**, *158*, 73−149.
(5) Turro, N. J.; Kleinman, M. H.; Karatekin, E. *Angew. Chem., Int. Ed. Engl.* **2000**, *39*, 4436−4461.
(6) Armaroli, N. *Photochem. Photobiol. Sci.* **2003**, *2*, 73−87.
(7) Deisenhofer, J.; Michel, H. *Science* **1989**, *245*, 1463−1473.
(8) Schmidt-Mende, L.; Fechtenkotter, A.; Müllen, K.; Moons, E.; Friend, R. H.; MacKenzie, J. D. *Science* **2001**, *293*, 1119−1122.
(9) Garcia, C. G.; De Lima, J. F.; Iha, N. Y. M. *Coord. Chem. Rev.* **2000**, *196*, 219−247.
(10) Becker, S.; Ego, C.; Grimsdale, A. C.; List, E. J. W.; Marsitzky, D.; Pogantsch, A.; Setayesh, S.; Leising, G.; Müllen, K. *Synth. Met.* **2001**, *125*, 73−80.
(11) Angadi, M. A.; Gosztola, D.; Wasielewski, M. R. *J. Appl. Phys.* **1998**, *83*, 6187−6189.
(12) Gust, D.; Moore, T. A.; Moore, A. L.; Lee, S. J.; Bittersmann, E.; Luttrull, D. K.; Rehms, A. A.; Degraziano, J. M.; Ma, X. C.; Gao, F.; Belford, R. E.; Trier, T. T. *Science* **1990**, *248*, 199−201.
(13) Gust, D.; Moore, T. A. *Science* **1989**, *244*, 35−41.
(14) Wasielewski, M. R. *Chem. Rev.* **1992**, *92*, 435.
(15) Vögtle, F.; Stoddart, J.; Shibasaki, M. In *Electron and Energy Transfer, in Stimulating Concepts in Chemistry*; Paddon-Row, M. N., Ed.; Wiley-VCH: New York, 2000; pp 267−291.
(16) Gust, D.; Moore, T. A.; Moore, A. L. *Acc. Chem. Res.* **1993**, *26*, 198−205.
(17) Gust, D.; Moore, T. A.; Moore, A. L. *Acc. Chem. Res.* **2001**, *34*, 40−48.
(18) Demmig, S.; Langhals, H. *Chem. Ber.-Rec.* **1988**, *121*, 225−230.
(19) Langhals, H. *Heterocycles* **1995**, *40*, 477−500.
(20) Muthukumaran, K.; Loewe, R. S.; Kirmaier, C.; Hindin, E.; Schwatz, J. K.; Sazanovich, I. V.; Diers, J. R.; Bocian, D. F.; Holton, D.; Lindsey, J. S. *J. Phys. Chem. B* **2003**, 3431−3442.
(21) Thelakkat, M.; Poesch, P.; Schmidt, H.-W. *Macromolecules* **2001**, *34*, 7441−7447.
(22) Belfield, K. D.; Schafer, K. J.; Alexander, M. D., Jr. *Chem. Mater.* **2000**, *12*, 1184−1186.
(23) Gregg, B. A.; Sprague, J.; Peterson, M. W. *J. Phys. Chem. B* **1997**, *101*, 5362−5369.
(24) Ferrere, S.; Zaban, A.; Gregg, B. A. *J. Phys. Chem. B* **1997**, *101*, 4490−4493.
(25) Ferrere, S.; Gregg, B. A. *New J. Chem.* **2002**, *26*, 1155−1160.
(26) Neuteboom, E. E.; Beckers, E. H. A.; Meskers, S. C. J.; Meijer, E. W.; Janssen, R. A. J. *Org., Biomol. Chem.* **2003**, *1*, 198−203.
(27) Schenning, A. P. H. J.; van Herrikhuyzen, J.; Jonkheijm, P.; Chen, Z.; Würthner, F.; Meijer, E. W. *J. Am. Chem. Soc.* **2002**, *124*, 10252−10253.
(28) Würthner, F. *Nach. Chem.* **2001**, 1284−1290.
(29) Würthner, F.; Thalacker, C.; Sautter, A. *Adv. Mater.* **1999**, *11*, 754−758.
(30) Würthner, F.; Thalacker, C.; Sautter, A.; Schärtl, W.; Ibach, W.; Hollricher, O. *Chem. Eur. J.* **2000**, *6*, 3871−3886.
(31) Würthner, F.; Thalacker, C.; Diele, S.; Tschierske, C. *Chem. Eur. J.* **2001**, *7*, 2245−2253.
(32) Thalacker, C.; Würthner, F. *Adv. Funct. Mater.* **2002**, *12*, 209−218.
(33) Dobrawa, R.; Würthner, F. *Chem. Commun.* **2002**, 1878−1879.
(34) Herrmann, A.; Weil, T.; Sinigersky, V.; Wiesler, U. M.; Vosch, T.; Hofkens, J.; De Schryver, F. C.; Müllen, K. *Chem. Eur. J.* **2001**, *7*, 4844−4853.
(35) Lor, M.; Thielemans, J.; Viaene, L.; Cotlet, M.; Hofkens, J.; Weil, T.; Hampel, C.; Müllen, K.; Verhoeven, J. W.; Van der Auweraer, M.; De Schryver, F. C. *J. Am. Chem. Soc.* **2002**, *124*, 9918−9925.
(36) Schweitzer, G.; Gronheid, R.; Jordens, S.; Lor, M.; De Belder, G.; Weil, T.; Reuther, E.; Müllen, M.; De Schryver, F. C. *J. Phys. Chem. A* **2003**, *107*, 3199−3207.
(37) Jordens, S.; De Belder, G.; Lor, M.; Schweitzer, G.; Van der Auweraer, M.; Weil, T.; Reuther, E.; Müllen, L.; De Schryver, F. C. *Photochem. Photobiol. Sci.* **2003**, *2*, 177−186.
(38) Ford, W. E.; Kamat, P. V. *J. Phys. Chem.* **1987**, *91*, 6373−6380.
(39) Zeiny, E.; Eldaly, S. A.; Langhals, H. *J. Phys. Chem.* **1988**, *92*, 4565−4568.
(40) Ford, W. E.; Hiratsuka, H.; Kamat, P. V. *J. Phys. Chem.* **1989**, *93*, 6692−6696.
(41) Lee, S. K.; Zu, Y. B.; Herrmann, A.; Geerts, Y.; Müllen, K.; Bard, A. J. *J. Am. Chem. Soc.* **1999**, *121*, 3513−3520.
(42) Oneil, M. P.; Niemczyk, M. P.; Svec, W. A.; Gosztola, D.; Gaines, G. L.; Wasielewski, M. R. *Science* **1992**, *257*, 63−65.

(43) Würthner, F.; Sautter, A. *Chem. Commun.* **2000**, 445−446.
(44) Würthner, F.; Sautter, A. *Org. Biomol. Chem.* **2003**, *1*, 240−243.
(45) You, C.-C.; Würthner, F. *J. Am. Chem. Soc.* **2003**, *125*, 9716−9725.
(46) Hawker, C. J.; Frechet, J. M. J. *J. Chem. Soc., Perkin Trans. 1* **1992**, 2459−2469.
(47) Moore, J. S.; Stupp, S. I. *Macromolecules* **1990**, *23*, 65−70.
(48) Gvishi, R.; Reisfeld, R.; Burshtein, Z. *Chem. Phys. Lett.* **1993**, *213*, 338−344.
(49) Liu, D.; De Feyter, S.; Cotlet, M.; Stefan, A.; Wiesler, U.-M.; Herrmann, A.; Grebel-Koehler, D.; Qu, J.; Müllen, K.; De Schryver, F. C. *Macromolecules* **2003**, *36*, 5918−5925.
(50) Murov, S.; Carmichael, I.; Hug, G. L. *Handbook of Photochemistry*, 2nd ed.; Marcel Dekker: New York, 1993.
(51) Pullerits, T.; Hess, S.; Herek, J. L.; Sundstrom, V. *J. Phys. Chem. B* **1997**, *101*, 10560−10567.
(52) Kawai, K.; Takada, T.; Tojo, S.; Ichinose, N.; Majima, T. *J. Am. Chem. Soc.* **2001**, 12688−12689.
(53) Foggi, P.; Pettini, L.; Santa, I.; Righini, R.; Califano, S. *J. Phys. Chem.* **1995**, *99*, 7439−7445.
(54) De Belder, G.; Jordens, S.; Lor, M.; Schweitzer, G.; De, R.; Weil, T.; Herrmann, A.; Wiesler, U. K.; Müllen, K.; De Schryver, F. C. *J. Photochem. Photobiol. A: Chem.* **2001**, *145*, 61−70.
(55) Lakowicz, J. R. *Principles of Fluorescence Spectroscopy*, 2nd ed.; Kluwer Academic/Plenum Publishers: New York, 1999.
(56) Förster, T. *Ann. Phys.* **1948**, 55−75.
(57) Stryer, L.; Haugland, R. P. *Proc. Natl. Acad. Sci. U.S.A.* **1967**, 719−726.
(58) Kroon, J.; Oevering, H.; Verhoeven, J. W.; Warman, J. M.; Oliver, A. M.; Paddon-Row, M. N. *J. Am. Chem. Soc.* **1993**, *115*, 5−5069.
(59) Marcus, R. A. *J. Chem. Phys.* **1956**, *24*, 966.
(60) Marcus, R. A.; Sutin, N. *Biochim. Biophys. Acta* **1985**, *811*, 265.
(61) Perrin, D. D.; Armarego, W. L. F. *Purification of Laboratory Chemicals*, 2nd ed.; Pergamon: Oxford, U.K., 1980.
(62) Eaton, D. F. *Pure Appl. Chem.* **1988**, *60*, 1107.
(63) Timmermans, J. *Physico-Chemical Constants of Pure Organic Compounds*; Elsevier: Amsterdam, 1965; Vols. I−II.